

The Mu2e experiment at Fermilab: Design and status

R. DONGHIA on behalf of the Mu2e COLLABORATION^(*)

INFN-National Laboratory of Frascati and Roma Tre University - Rome, Italy

received 16 September 2017

Summary. — The Mu2e experiment at Fermilab will search for coherent, neutrinoless conversion of negative muons into electrons in the field of an aluminum nucleus. The dynamics of such charged lepton flavour violating (CLFV) process is a two-body decay, resulting in a mono-energetic electron with an energy slightly below the muon rest mass. If no events are observed in three years of running, Mu2e will set an upper limit on the ratio between the conversion and the capture rates $R_{\mu e}$ of $\leq 6 \times 10^{-17}$ (@90% C.L.). This will improve the current limit of four order of magnitudes with respect to the previous best experiment. Mu2e complements and extends the current search for $\mu \rightarrow e\gamma$ decay at MEG as well as the direct searches for new physics at the LHC. Indeed, such a CLFV process probes new physics at a scale inaccessible to direct searches at either present or planned high energy colliders. Observation of a signal will be a clear evidence for new physics beyond the Standard Model. To search for the muon conversion process, a very intense pulsed beam of negative muons ($\sim 10^{10} \mu/s$) is stopped on an aluminum target inside a very long solenoid where the detector is also located. The Mu2e detector is composed of a straw tube tracker and an electromagnetic calorimeter consisting of arrays of CsI crystals. An external veto for cosmic rays is surrounding the detector solenoid. In 2016, Mu2e has passed the final approval stage from DOE and has started its construction phase. Data collection is planned for the end of 2021. An overview of the physics motivations for Mu2e, the current status of the experiment and design of the muon beam-line and the detector is presented.

1. – Charged Lepton Flavor Violation and muon to electron conversion

Within the Standard Model (SM), transitions in the lepton sector between charged and neutral particles preserve flavor, since the neutrinos are considered massless. Even considering the discovery of neutrino oscillations, in the minimal extension of SM, the predicted branching ratios of Charged Lepton Flavor Violation (CLFV) processes in the muon sector are smaller than 10^{-50} , unreachable by the current particle accelerators.

^(*) Mu2e Collaboration, <http://mu2e.fnal.gov/collaboration.shtml>

Any experimental detection of CLFV would be a clear signature of new physics (NP), however no such signal has yet been seen. One of the most promising processes for probing CLFV is the coherent muon conversion in the field of a nucleus, $\mu N \rightarrow e N$. In this process the nucleus is left intact and the resulting electron has a monochromatic energy slightly below the muon rest mass (~ 104.96 MeV), due to the nucleus recoil.

The Mu2e experiment [1] is designed to improve the current limit on the conversion rate, $R_{\mu e}$, by 4 orders of magnitude over the SINDRUM II experiment [2]. The $R_{\mu e}$ rate is defined as the ratio between the number of electrons from the conversion process and the number of captured muons,

$$R_{\mu e} = \frac{\mu^- N(Z, A) \rightarrow e^- N(Z, A)}{\mu^- N(Z, A) \rightarrow \nu_\mu N(Z-1, A)} < 6 \times 10^{-17} \text{ (at 90\% C.L.)},$$

where, in the Mu2e case, $N(Z, A)$ is an aluminum nucleus.

Many NP scenarios, like SUSY, Leptoquarks, Heavy Neutrinos, GUT, Extra Dimensions or Little Higgs, predict significantly enhanced values for $R_{\mu e}$, at a level accessible by the Mu2e sensitivity [3].

A model independent description of the CLFV transitions, for NP models, is provided by an effective Lagrangian [4] where the different processes are divided in dipole amplitudes and contact term operators. The $\mu \rightarrow e \gamma$ decay is mainly sensitive to the dipole amplitude, while $\mu \rightarrow e$ conversion and $\mu \rightarrow 3e$ receive contributions also from the contact interactions. It is possible to parametrise the interpolation between the two amplitudes by means of two parameters [4]: Λ , which sets the mass scale, and κ , which governs the ratio of the four fermion to the dipole amplitude. For $\kappa \ll 1$ ($\gg 1$) the dipole-type (contact) operator dominates. Figure 1 summarises the power of different searches to explore this parameter space [5].

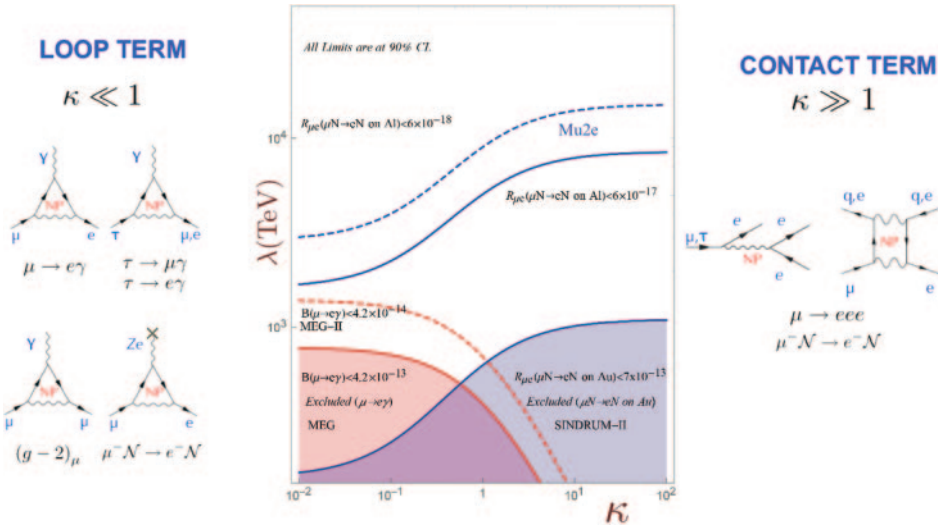


Fig. 1. – Sensitivity of $\mu \rightarrow e \gamma$, $\mu \rightarrow e$ transition and $\mu \rightarrow 3e$ to the scale of new physics Λ as a function of the parameter κ . The shaded areas are excluded by present limits. On the left (right) side, the dipole (contact) diagrams are shown for the different processes.

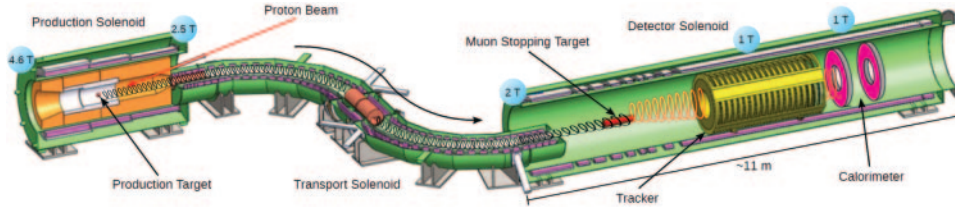


Fig. 2. – Layout of the Mu2e experiment.

Present experimental limits already excluded the energy scale up to $\Lambda < 700$ TeV, setting serious constraints on SM extensions. The interpretation of an eventual direct observation of NP at LHC will have to take into account precise measurements (or constraints) from MEG [6] and Mu2e: the comparison between these determinations will help pin down the underlying theory.

2. – The Mu2e experimental apparatus

The Mu2e apparatus consists of three superconductive solenoid magnets, as shown in fig. 2: the Production Solenoid (PS), the Transport Solenoid (TS) and the Detector Solenoid (DS).

To reach the sensitivity goal $R_{\mu e} < 6 \times 10^{-17}$ at 90% C.L., about 10^{18} stopped muons are needed.

Muons are produced using 8 GeV protons from the Fermilab accelerator complex, which provides a sequence of 200 ns wide micro-bunches separated by $1.7 \mu\text{s}$. The beam period is roughly twice the muon mean lifetime in Al nucleus, $\tau_{Al} = 864$ ns. This particular beam structure, as shown in fig. 3, allows Mu2e to use a delayed selection windows to suppress the prompt background coming from proton interactions.

The proton beam interacts in the PS with a tungsten target, producing mostly pions and muons. The gradient field in the PS increases from 2.5 to 4.6 T in the same direction of the incoming beam and opposite to the outgoing muon beam direction. This gradient field works as a magnetic lens to focus charged particles into the transport channel.

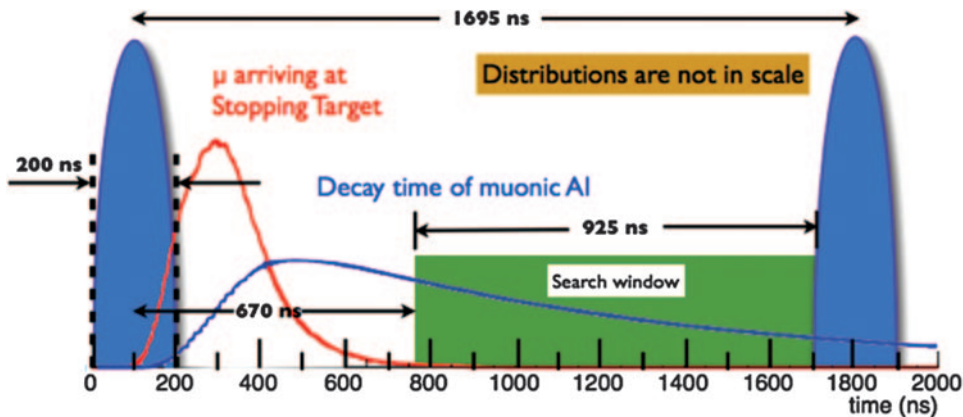


Fig. 3. – The Mu2e spill cycle for the proton on target pulse (blue distributions) and the delayed selection window (green) that allows an effective elimination of the prompt background.

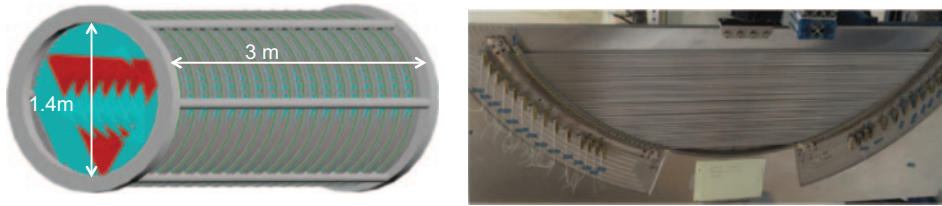


Fig. 4. – Left: sketch of the Mu2e straw tracker system. Right: picture of the first prototype built for straw tube panel.

The focused beam is constituted by muons, pions and a small number of protons and antiprotons. When the beam passes through the S-shaped TS, low momentum negative charged particles are selected and delivered to the aluminum stopping target foils in the DS. Electrons from the μ -conversion (CE) in the stopping target are captured by the magnetic field in the DS and transported through the Straw Tube Tracker, which reconstructs the CE trajectory and its momentum. The CE then strikes the Electromagnetic Calorimeter, which provides independent measurements of the energy, the impact time and the position. Both detectors operate in a 10^{-4} Torr vacuum and in an uniform 1 T axial field.

A Cosmic Ray Veto (CRV) system covers the entire DS and half of the TS, as shown in fig. 5 (right).

Measurement of the total number of captured muons is provided by a high purity germanium detector, via the observation of the X-rays resulting from the nuclear capture.

Additional details on the Mu2e experimental apparatus can be found in the Technical Design Report [1].

3. – The Mu2e detector

The tracking detector is made of low mass straw drift tubes oriented transversally to the solenoid axis. The detector consists of about 20000 straw tubes arranged in 18 stations, as shown in fig. 4 (left). Each tube is 5 mm in diameter and contains a $25\ \mu\text{m}$ sense wire. The straw walls are made out of Mylar and have a thickness of $15\ \mu\text{m}$.

The gas used is a 80:20 mixture of Argon- CO_2 . The tracker is around 3 m long and measures the momenta of the charged particles from the reconstructed trajectories using the hits detected in the straw.

In fig. 4 (right), an example of the first panel prototype built is shown.

A circular inner hole inside the tracker allows it to be insensitive to the large flux of charged particles below 55 MeV/c and only particles with $P_T > 90$ MeV leave enough hits to form a reconstructible trajectory.

Indeed the detectors acceptance is optimised to identify ~ 100 MeV electrons.

The electromagnetic calorimeter [7] consists of two disks of scintillating crystals and is placed downstream the tracker. Each disk is composed by 674 pure CsI crystals of $(34 \times 34 \times 200)\ \text{mm}^3$ dimensions, each readout by two UV-extended Silicon Photomultipliers (SiPM) [8, 9].

In fig. 5 (left) a drawing of these two disks is shown. Similarly to the tracker, the inner circular hole allows it to be insensitive to electrons up to 55 MeV/c momenta.

The calorimeter aims are to provide a powerful particle identification between muons and electrons, an independent trigger system and a seed for tracking in a complicated reconstruction environment.

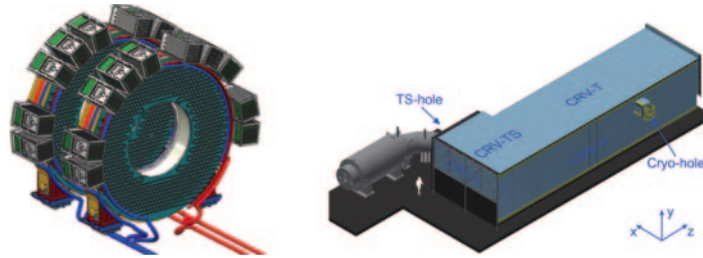


Fig. 5. – Left: CAD drawings of the calorimeter disks. Calorimeter innermost (outermost) radius is of 350 mm (600 mm). Layout of the FEE and digitization crates is also shown. Right: schematic drawing CRV system, covering part of the TS and the entire TS.

The calorimeter particle identification provides a good separation between CEs and muons un-vetoed by the CRV and mimicking the signal. The required muon rejection factor is provided with 95% efficiency on the signal, combining the time of flight difference between the tracker track and the calorimeter cluster with the E/p ratio.

In order to satisfy these requirements, the calorimeter has to reach an energy resolution of $O(5\%)$, a time resolution less than 500 ps and a position resolution better than 1 cm for 100 MeV electrons. The selected crystals should also be radiation hard to a dose of 100 krad and a fluency up to 10^{12} n/cm². The photosensors are shielded by the crystals themselves and need only sustain a fluency up to 3×10^{11} n/cm².

One major background source for Mu2e is related to cosmic ray muons faking CEs when interacting with the detector materials. In order to reduce their contributions to below 0.1 event in the experiment lifetime, the CRV system is required to achieve a vetoing efficiency of at least 99.99% for cosmic ray tracks while withstanding an intense radiation environment. The basic element of the CRV is constituted by four staggered layers of scintillation bars, each having two embedded Wavelength Shifting Fibres readout by means of (2×2) mm² SiPM.

4. – Expected background

When negative muons stop in the aluminum target, they are captured in an atomic excited state. The resultant muonic atoms persist with a lifetime of 864 ns, decaying in orbit (DIO) 39% of the time while capturing on the nucleus the other 61% of the time. Low energy photons, neutrons and protons are emitted in the nuclear capture process and constitute an environmental background that produces an ionization dose and a neutron fluency on the detection systems as well as an accidental occupancy for the reconstruction program.

The kinematic limit for the muon decay in vacuum is at about 54 MeV, but the nucleus recoil generates a long tail that has the endpoint exactly at the conversion electron energy.

For this reason, DIO electrons are an irreducible background that have to be distinguished by the mono-energetic CE. The finite tracking resolution and the positive reconstruction tail has a large effect on the falling spectrum of the DIO background that translates in a residual contamination in the signal region.

Estimate of other backgrounds are presented in table I for a total background contribution of 0.37 events.

TABLE I. – *Expected background list as evaluated by full simulation.*

Category	Background process	Estimated yield (events)
intrinsic	decay in orbit (DIO)	0.199 ± 0.092
	muon capture (RMC)	0.000 ± 0.004
late arriving	pion capture (RPC)	0.023 ± 0.006
	muon decay in flight	< 0.003
	pion decay in flight	0.001 ± 0.001
	beam electrons	0.003 ± 0.001
miscellaneous	antiproton induced	0.047 ± 0.024
	cosmic rays	0.092 ± 0.020
total		0.37 ± 0.10

5. – Conversion electron reconstruction

At the CE energy the momentum resolution is dominated by fluctuations in the energy loss in the target, multiple scattering and bremsstrahlung in the tracker. By performing a full simulation of the tracker, a pattern recognition and a Kalman fitter for the tracking we obtain: a CE reconstruction efficiency of 9% for good quality tracks and at least 25 hits/track. The resolution is well parametrised by a Crystal Ball function with a negative bremsstrahlung tail, a Gaussian core of 116 keV and a long exponential positive resolution tail.

Figure 6 (right) shows the signal and background distributions as seen by a full simulation of the experiment (pileup included) in the following conditions: i) 3.6×10^{20}

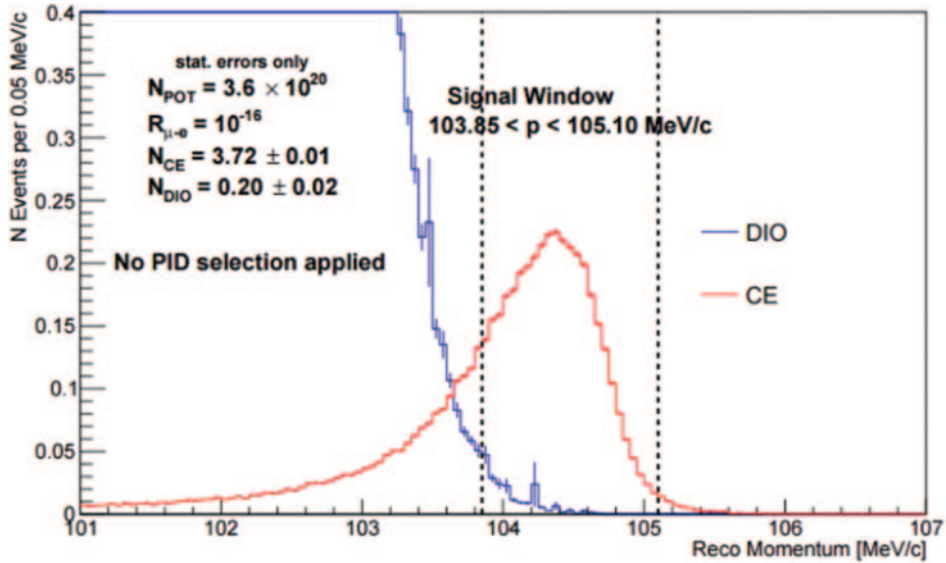


Fig. 6. – Full simulation of DIO and CE events for an assumed $R_{\mu e}$ of 10^{-16} .

proton on target, ii) 6×10^{17} stopped muons and iii) a $R_{\mu e}$ of 10^{-16} . After maximising signal over background, the best selection corresponds to counting events in a momentum window between 103.75 and 105 MeV/c. A DIO contribution of 0.199 events is estimated and 3.5 candidates are observed. This counting corresponds to setting a limit on $R_{\mu e}$ below 6×10^{-17} at 90% C.L., in good agreement with the experimental goal.

An important step for this measurement is the tracker calibration. To accurately predict the DIO rate, we should calibrate the tracker momentum, determining the shifts, the scale and the resolution of the measured momentum compared to the true one. After a basic calibration based on construction and installation survey data, the calibration will be based both on the usage of the lower momentum high statistic DIO sample itself and on independent processes of low energy two body decay, such as the one from stopped π^+ on target undergoing the $\pi \rightarrow e\nu$ decay. Selecting the positive pions will help to avoid nuclear capture but asks for reversing the momentum selection in the TS. Moreover, the data have to be collected at shorter rate and an extrapolation from lower energies to the conversion endpoint is needed.

6. – Conclusions and perspectives

The Mu2e experiment design and construction is proceeding well and it is on schedule to be commissioned with beam for the end of 2021. Its goal is to probe CLFV with a single event sensitivity of 2.5×10^{-16} to set an upper limit on the conversion rate $< 6 \times 10^{-17}$ at 90% C.L., improving over the previous experimental limit by four orders of magnitude.

A Mu2e second phase is already planned with the goal of increasing the sensitivity of an additional factor of 10. This can be obtained aiming to get a higher beam intensity and a detector that withstands this intensity and is able to handle the accidental activity coming from muon capture. In this context, only the option based on the new Proton Improvement Plan, PIP-2 [10], is being studied.

* * *

This work was supported by the EU Horizon 2020 Research and Innovation Programme under the Marie Skłodowska-Curie Grant Agreement No. 690835.

REFERENCES

- [1] BARTOSZEK L. *et al.*, *Mu2e Technical Design Report*, arXiv:1501.05241.
- [2] BERTL W. *et al.*, *Eur. Phys. J. C*, **47** (2006) 337.
- [3] RAIDAL M. *et al.*, *Eur. Phys. J. C*, **57** (2008) 13.
- [4] DE GOUVEA A. *et al.*, *Prog. Part. Nucl. Phys.*, **71** (2013) 75, arXiv:1303.4097.
- [5] BERNSTEIN R. and COOPER P., *Phys. Rep.*, **532** (2013) 27.
- [6] BALDINI A. M. *et al.*, *Eur. Phys. J. C*, **76** (2016) 434.
- [7] ATANOV N. *et al.*, *Nucl. Instrum. Methods A*, **824** (2016) 695, arXiv:1608.02652.
- [8] ANGELUCCI M. *et al.*, *Nucl. Instrum. Methods A*, **824** (2016) 678, arXiv:1606.07110.
- [9] ATANOV O. *et al.*, *JINST*, **12** (2017) P05007, arXiv:1702.03720.
- [10] <http://pip2.fnal.gov>